Stability and Placement of Ag/AgCl Quasi-Reference Counter Electrodes in Confined Electrochemical Cells

Cameron L. Bentley[*]*, David Perry, Patrick R. Unwin*[*]

Department of Chemistry, University of Warwick, Coventry CV4 7AL, United Kingdom

*C.Bentley.1@warwick.ac.uk, +44 (0)24 7657 2882 (C.L.B.); P.R.Unwin@warwick.ac.uk, +44 (0)24 7652 3264 (P.R.U.)

Abstract. Nanoelectrochemistry is an important and growing branch of electrochemistry that encompasses a number of key research areas, including (electro)catalysis, energy storage, biomedical/environmental sensing and electrochemical imaging. Nanoscale electrochemical measurements are often performed in confined environments over prolonged experimental timescales with non-isolated quasi-reference counter electrodes (QRCEs) in a simplified two-electrode format. Herein, we consider the stability of commonly used Ag/AgCl QRCEs, comprising an AgCl-coated wire, in a nanopipet configuration, which simulates the confined electrochemical cell arrangement commonly encountered in nanoelectrochemical systems. Ag/AgCl QRCEs possess a very stable reference potential even when used immediately after preparation, and when deployed in Cl^- free electrolyte media (*e.g.*, 0.1 M $HClO_4$) in the scanning ion conductance microscopy (SICM) format, drift by only *ca.* 1 mV h^{-1} on the several hours timescale. Furthermore, contrary to some previous reports, when employed in a scanning electrochemical cell microscopy (SECCM) format (meniscus contact with a working electrode surface), Ag/AgCl QRCEs do not cause fouling of the surface (*i.e.*, with soluble redox by-products, such as Ag^+) on at least the 6 hours timescale, as long as suitable precautions with respect to electrode handling and placement within the nanopipet are observed. These experimental observations are validated through finite element method (FEM) simulations, which consider Ag^+ transport within a nanopipet probe in the SECCM and SICM configurations. These results confirm that Ag/AgCl is a stable and robust QRCE in confined electrochemical environments, such as in nanopipets used in SICM, for nanopore measurements, for printing and patterning, and in SECCM, justifying the widespread use of this electrode in the field of nanoelectrochemistry and beyond.

Introduction

Significant advances in fabrication and characterization methods have seen modern electrochemical science being impacted massively by the nanotechnology revolution, effectively giving rise to a new branch of study known as 'nanoelectrochemistry'.[1,2] In nanoelectrochemistry, the dimensions of the electrochemical probe or sensor (*e.g.*, nanopore, nanogap, nanopipet or nanoelectrode) is reduced to the nanoscale in order to study phenomena at the 1 to 100 nm length scale. This has enabled fundamental studies to be carried out at the 'single entity level', where individual nanoparticles[1-3], vesicles[4,5], molecules[6,7], cells[8-10] *etc.* are detected and/or characterized using either 'static' (*e.g.*, DNA sensing[11], single nanoparticle impact studies[12-14] *etc.*) or 'dynamic' (*e.g.*, high-resolution electrochemical imaging[15-17]) electrochemical probes.

As well as small length-scales, nanoelectrochemistry is increasingly performed in confined volumes, and the high mass-transport rates intrinsic to the nanoscale give rise to a whole new set of experimental considerations/complications when compared to traditional 'macroscopic' electrochemistry.[1,2] In nanoelectrochemistry large datasets are often required for statistical significance (*e.g.*, in single molecule/nanoparticle detection[1-3,6,7,11-14]) and/or to ensure areas of sufficient size are mapped in electrochemical imaging, which can result in prolonged measurement times.[18-21] Furthermore, nanoscale experiments are usually carried out in a simplified two-electrode format, where the working electrode (WE) is balanced by a single 'quasi-reference counter electrode' (QRCE), which is justified when the measured current is small enough (*e.g.*, fA to nA) to prevent significant polarization of the reference potential. Due to size, cost and complexity constraints, conventional fritted QRCEs are not usually employed in nanoscale electrochemical systems, with non-isolated QRCEs (*e.g.*, Ag/AgCl) often being used instead.

A major consequence of prolonged measurement times is that the stability of the defined reference potential (*i.e.*, QRCE potential) is of utmost importance in order to ensure high-fidelity data. In addition, QRCE placement with respect to the WE (or biological entity, as in live cell imaging[8-10,22,23]) is also an important consideration, with recent articles reporting artifacts at WEs arising from Ag/AgCl contamination from QRCEs in confined electrochemical cells.[24,25] For example, Perera and Rosenstein[25] reported on the *in situ* generation of metallic nanoparticles in a nanopipet contact format (also known as scanning electrochemical cell microscopy, SECCM[17,26]), which they attributed to the generation of soluble redox by-products at the Ag/AgCl or Cu/$CuCl_2$ QRCE that was used in their studies. In that report, the authors claim to have observed QRCE contamination-induced effects after only 40 minutes of operation with a range of WE materials [glassy carbon (GC) and platinum] and electrolytes (chloride, phosphate and sulfate). This observation has far-reaching consequences beyond nanoelectrochemistry, as non-isolated Ag/AgCl quasi-reference electrodes are used extensively in electrochemical lab-on-a-chip devices,[24] in screen printed electrodes,[27] as well as in nanopore devices,[11,28] and nanopipet imaging techniques, such as scanning ion conductance microscopy (SICM).[29,30]

Although any possibility of contamination from QRCEs can be entirely avoided by using non-fouling QRCEs such as palladium-hydrogen (Pd-H_2)[19-21], a simple 'back-of-the-envelope' calculation of diffusion time on the cm length-scale ($t_\mathrm{d} = L^2/2D$, where t_d is the diffusion time, L is the diffusion length and D is the diffusion coefficient)[31] indicates that fouling should only be an issue on the tens of hours timescale, with careful positioning of the QRCE. However, in light of the recent reports alluded to above, and given the increasing use of simple AgCl-Ag wires as QRCEs in various applications, herein we consider the stability and placement of Ag/AgCl QRCEs, using a nanopipet configuration (*vide infra*) to emulate a confined electrochemical cell. Experiments, supported by complementary finite element

method (FEM) simulations, demonstrate that Ag/AgCl QCREs can be used for long times without any problems from contamination or potential instability.

Experimental Section

Chemical Reagents and Electrode Materials. Perchloric acid ($HClO_4$, Sigma-Aldrich, 70%) and potassium chloride (KCl, Sigma-Aldrich) were used as supplied by the manufacturer. All solutions were prepared with deionized water (resistivity = 18.2 MΩ.cm at 25°C, Integra HP, Purite, U.K.). The GC substrate (HTW Hochtemperatur-Werkstoffe GmbH, Germany) was polished with an aqueous slurry of 0.05 μm Al_2O_3 (Buehler, U.S.A.) prior to use. The Ag/AgCl QRCE was prepared by abrading a 0.25 mm diameter annealed silver wire (Goodfellow, U.K., 99.99%) with P1200 sandpaper (Buehler, U.S.A.), sonicating and then anodizing in a saturated solution of KCl (*vs.* a Pt wire counter electrode). It should be noted that the stability of Ag/AgCl electrodes can be further improved by "aging", which was not carried out here (the Ag/AgCl QRCEs were used immediately after preparation).[32]

Electrochemical Experiments. In the QRCE stability set of experiments, an Ag/AgCl QRCE was placed into a single-barreled nanopipet probe (tip diameter, $d_t \approx 500$ nm) that was filled with electrolyte solution (0.1 M $HClO_4$). The tip of the probe was subsequently placed into an electrolyte bath (also 0.1 M $HClO_4$), and the potential of the Ag/AgCl QRCE was monitored against a commercial Ag/AgCl reference electrode (3.4 M KCl, ET072-1, eDAQ, Australia), using the 'open circuit potential' module on a FAS2 Femtostat (Gamry Instruments, U.S.A.). In a separate set of experiments, currents of ±1 nA were applied at the probe ($d_t \approx 100$ nm) in a 3 electrode format (an Ag/AgCl wire in bulk served as a counter electrode) using the 'chronopotentiometry' module on a FAS2 Femtostat.

The QRCE placement set of experiments were carried out in the SECCM format on a home-built electrochemical workstation.[26,33] Briefly, an Ag/AgCl QRCE was placed into a

single-barreled nanopipet probe ($d_t \approx 100$ nm) that was filled with electrolyte solution (0.1 M $HClO_4$) and mounted on an *xyz*-piezoelectric positioner (P-611.3S, Physik Instrumente, Germany). Note that the probe size used herein is mid-range between the smallest SECCM tips used ($d_t \approx 30$ nm)[19,21] and the ones of a few hundred nm, used routinely.[18,34-36] The nanopipet probe was positioned above the substrate surface using stepper motors (8303 Picomotor Actuator, Newport, U.S.A.) for coarse movement and the *xyz*-piezoelectric positioner for fine movement. During each approach, surface current (i_{surf}) was used as a feedback signal to detect when the meniscus cell had made contact with the WE surface. Note that the nanopipet itself never made contact with the WE surface.

Electrochemical measurements at the WE were made using a cyclic voltammetric "hopping" regime, as previously reported.[19,34] In brief, the nanopipet probe was approached to the WE surface at a series of predefined locations in a grid and, upon each landing, an independent cyclic voltammogram (CV) was recorded. For each CV, the potential was initially held at –0.7 V for 5 seconds (*ca.* –0.23 V *vs.* standard hydrogen electrode, SHE, sufficient to electro-deposit any Ag^+ by reduction to Ag at the diffusion-limited rate)[31], before cycling to +0.4 V at 0.1 V s^{-1} to electro-oxidatively strip Ag^+. For comparison, Perera and Rosenstein[25] continually cycled the potential between ±0.4 V vs. Ag/AgCl QRCE at 0.1 V s^{-1}. The hopping distance (*i.e.*, separation between each pixel) was set to 1 μm to ensure each CV was obtained on a 'fresh' GC surface (*i.e.*, each measurement was independent of the previous).

The entire SECCM set up was situated in an aluminum Faraday cage, equipped with heat sinks and vacuum panels to minimize thermal drift and noise. The Faraday cage was installed on an optical table (RS2000, Newport, U.S.A.) with automatic levelling isolators (Newport, S-2000A-423.5). The GC substrate (WE) was placed into an environmental control cell, which was continually purged with humidified air or argon (Ar, BOC gas, Pureshield, 99.998%). The potential of the QRCE was controlled, with respect to ground, and the current

flowing at the WE, held at a common ground, was measured using a home-built electrometer. A home-built 8th order (low-pass) brick-wall filter unit with a time constant (t_c) of 2 or 10 ms was utilized during data (current) acquisition. Data acquisition and instrumental control was carried out using an FPGA card (PCIe-7852R) controlled by a LabVIEW 2016 (National Instruments, U.S.A.) interface running the Warwick Electrochemical Scanning Probe Microscopy (WEC-SPM, *www.warwick.ac.uk/electrochemistry*) software.

The single-barreled nanopipet probes were fabricated from borosilicate glass filamented capillaries (GC120F-10, Harvard Apparatus, U.S.A.) using a CO_2-laser puller (P-2000, Sutter Instruments, U.S.A.). Pulling parameters ($d_t \approx 500$ *nm*): Line 1: HEAT 350, FIL 3, VEL 40, DEL 220, PUL -; Line 2: HEAT 350, FIL 3, VEL 40, DEL 180, PUL 100. Pulling parameters ($d_t \approx 100$ *nm*): Line 1: HEAT 350, FIL 3, VEL 30, DEL 220, PUL -; Line 2: HEAT 350, FIL 3, VEL 40, DEL 180, PUL 120. After the nanopipet probes were filled with the electrolyte solution (0.1 M $HClO_4$) using a MicroFil syringe (World Precision Instruments Inc., U.S.A.), a thin layer of silicone oil (DC 200, Sigma-Aldrich) was added on top in order to minimize evaporation. The freshly prepared QRCE was then inserted through the silicone layer, into the electrolyte solution, and mounted on the *xyz*-piezoelectric positioner, as described above. The distance between the end of the QRCE and nanopipet tip was *ca.* 3 cm. Images of the as-prepared probes, as well as additional experimental results are presented in the Supporting Information, Section S1. The time between completing the probe preparation and recording the first CV (*i.e.*, $t = 0$) was *ca.* 30 minutes.

After acquisition, the raw data were processed using the Matlab R2015b (8.6.0.267246, Mathworks, U.S.A.) software package. Data plotting was carried out using the OriginPro 2016 64bit (b9.3.226, OriginLab, U.S.A.) software package.

FEM Simulations. FEM simulations were performed in COMSOL Multiphysics v5.2a (COMSOL Inc., Sweden). Simulations encompassed a two-dimensional representation of a

nanopipet probe, with dimensions extracted from TEM images[37], situated above a substrate (WE) surface (SECCM simulations) or immersed in bulk solution (SICM simulations). In the SECCM simulations, three conditions were considered at the substrate surface: (*i*) the substrate is a no flux boundary, where there is no reaction occurring at the WE; (*ii*) $[Ag^+]_{surf} = 0$ (*i.e.*, Ag deposition occurs at the mass-transport controlled rate, the WE is an Ag^+ sink) and; (*iii*) initially a no flux boundary condition and then $[Ag^+]_{surf} = 0$ after 2, 5 or 20 hours (*i.e.*, Ag^+ is allowed to accumulate for a period of time before the reaction is 'switched on' at the mass-transport controlled rate). In the SICM simulations, a bias of +100 mV was applied at the electrode located in the nanopipet and the flux of Ag^+ at the orifice (tip) of the probe was calculated as a function of time. Further details are presented in the Supporting Information, Section S2.

Results and Discussion

Ag/AgCl quasi-reference counter electrode stability. As alluded to above, the stability of the QRCE potential is of the utmost importance, particularly at prolonged experimental measurement times. The potential adopted by an Ag/AgCl QRCE (E_{QRCE}) is dependent upon the activity of chloride (a_{Cl^-}) in solution:

$$E_{\mathrm{QRCE}} = E^0_{\mathrm{Ag/AgCl}} - \frac{RT}{F} \ln a_{\mathrm{Cl^-}} \qquad (1)$$

where E^0 is the standard electrode potential of the Ag/AgCl couple (0.2223 V vs. SHE)[31], R is the gas constant, T is the absolute temperature and F is Faraday's constant. a_{Cl^-} is approximated by $[Cl^-]$ and is fixed in Cl^- containing electrolyte solutions (thus, E_{QRCE} is expected to be stable). In Cl^- free electrolytes, the potential is set by the limited dissolution of sparingly soluble AgCl in the vicinity of the QRCE[38]

$$\mathrm{AgCl_{(s)}} \rightleftharpoons \mathrm{Ag^+_{(aq)}} + \mathrm{Cl^-_{(aq)}} \qquad (2)$$

$$E_{\mathrm{QRCE}} = E^0_{\mathrm{Ag/AgCl}} - \frac{RT}{2F} \ln K_{\mathrm{sp}} \qquad (3)$$

where K_{sp} is the solubility product of AgCl, equal to 1.77×10^{-10} at 298 K.[39] Writing Eq. (3) assumes that the dissolution of AgCl is fast compared to whatever diffusion rate prevails, which it is.[40,41] This relationship assumes that there is no Ag exposed in solution (the Ag/Ag^+ couple can shift the reference potential) and that there are no interfering species present (*e.g.*, Br^-).

In order to test the stability of the Ag/AgCl QRCEs under operational conditions, a nanopipet ($d_t \approx 500$ nm) configuration analogous to that used in SICM[29,30] or nanopore experiments[11,28] was chosen to simulate a confined electrochemical cell environment, as shown in Figure 1a. $HClO_4$ was chosen as the Cl^- free electrolyte because we have used it extensively in the past with both Ag/AgCl and Pd-H_2 QRCEs.[18,19,21,34] The potential of the Ag/AgCl QRCE was monitored in bulk solution against a commercial Ag/AgCl reference electrode over a 6.5 hour period, as shown in Figure 1b. Evidently, E_{QRCE} is very stable over prolonged experimental timescales even in this Cl^- free electrolyte, drifting by less than 10 mV over the 6.5 hour period (*ca.* 1.4 mV h^{-1}).

It should be noted that in 'real' SICM or dual-barrel SECCM experiments[30,33], the QRCE is biased in order to generate an ionic current typically on the order of ±1 nA. Thus, in order to investigate the stability of Ag/AgCl QRCEs over time in a 'typical use' case, a second set of experiments were carried out, again in a nanopipet configuration ($d_t \approx 100$ nm, closer in size to the probes used in actual SICM experiments[22,37]), except this time, constant currents of 0 (*i.e.*, 'open circuit potential', OCP), +1 and –1 nA were applied at the tip periodically in 20 minute intervals over a 6.5 hour period (*i.e.*, 7 individual measurements were performed under each condition), as shown in Figure 1c. Evidently, E_{QRCE} is very stable even when biased at *ca.* ±30 mV (*i.e.*, 'typical use' conditions) over prolonged experimental timescales, drifting by *ca.* 5 mV over a 6.5 hour period (*ca.* 0.8 mV h^{-1}).

Recent work by us demonstrated how large hopping mode SECCM[19,21] and SICM[20] scans with thousands of pixels can be completed in less than an hour, meaning that drift of *ca.*

1 mV h^{-1} is effectively negligible on this experimental timescale. Earlier SECCM studies are also made on a timescale of tens of minutes, for which this level of potential drift is negligible.[38,42] Finally, it is worth noting that this work was performed with freshly prepared Ag/AgCl electrodes; there is scope it further improve the stability of the QRCE potential through "aging" procedures before use, as reported elsewhere.[32]

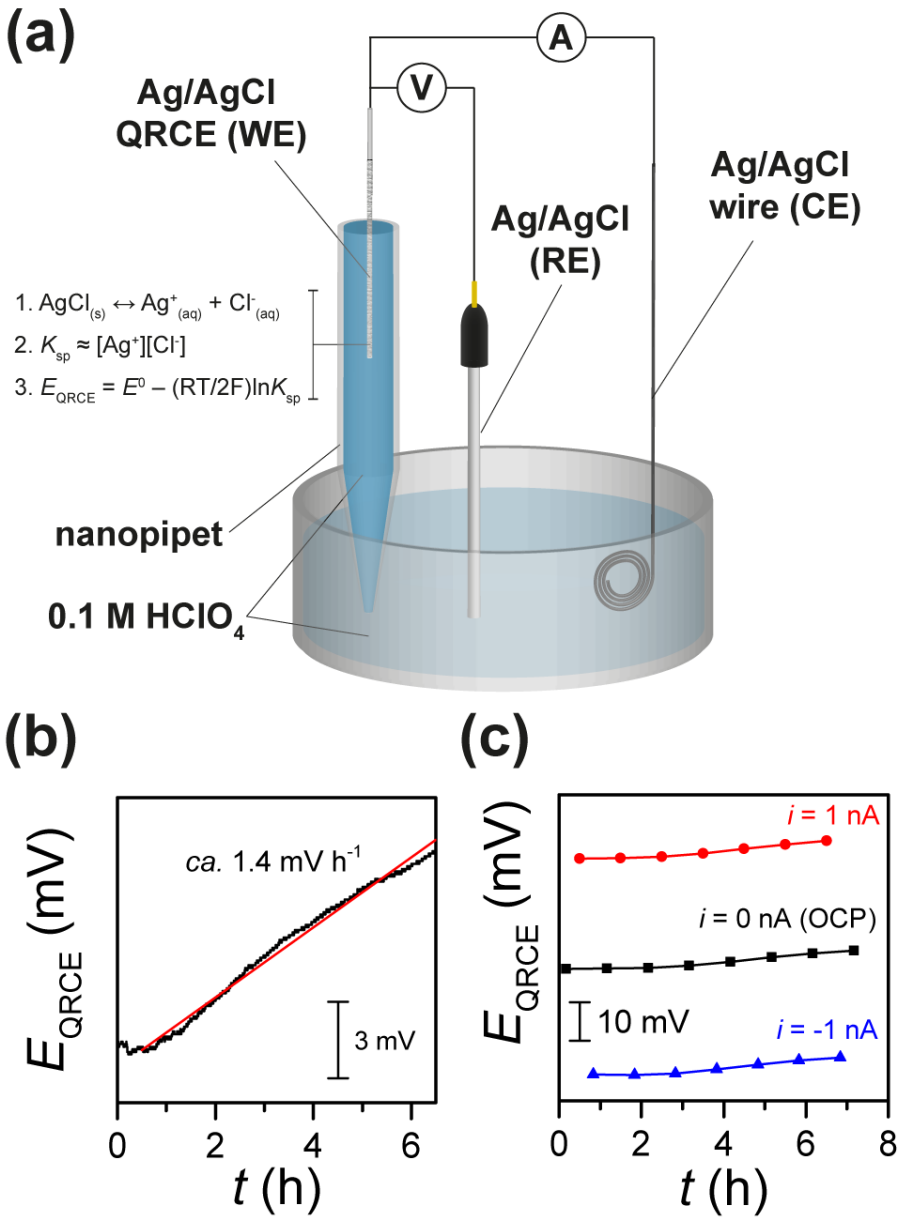

Figure 1. (a) Schematic of the set up used to monitor the stability of E_{QRCE} over prolonged experimental timescales in a confined electrochemical cell (nanopipet probe) containing 0.1 M $HClO_4$. WE, RE and CE signify working, reference and counter electrodes, respectively. **(b)** Plot of E_{QRCE} at an applied current of zero (open circuit potential, OCP), monitored over a 6.5 hour time period. Also shown is a linear least-squares regression line (red trace) used to estimate the drift in E_{QRCE} with time (*ca.* 1.4 mV h^{-1}). **(c)** Plots of E_{QRCE} at currents of 0 nA (OCP, black trace), +1 nA (red trace) and –1 nA (blue trace), applied at the QRCE in the probe (WE) periodically in 20 minute intervals. d_t was 500 and 100 nm in **(b)** and **(c)**, respectively.

Ag/AgCl quasi-reference counter electrode placement. As alluded to above, QRCE placement within confined electrochemical cells is an important consideration due to the possibility of Ag/AgCl contamination at the WE.[24,25] Ag^+ and Cl^- are both electroactive species and are initially present in the vicinity of the QRCE due to the limited solubility of AgCl, as shown above in Eq. (2). This, in itself, is not a problem, except if Ag^+ and Cl^- are transported to the vicinity of the WE (substrate), where they may undergo reduction (Ag^+/Ag^0) and oxidation (Cl^-/Cl_2), respectively (depending on the applied potential), interfering with the redox processes of interest. This issue is expected to be exacerbated with prolonged measurement times in confined electrochemical cells.

In order to investigate the possibility of Ag/AgCl contamination under operational conditions in a confined electrochemical cell environment, measurements were performed in the SECCM format,[17,21,26] as shown schematically in Figure 2a. In this configuration, voltammetric measurements are performed in the confined area defined by the meniscus cell created between a pulled nanopipet ($d_t \approx 100$ *nm*) probe and substrate (WE) surface. A 'hopping mode' protocol has been used herein, in which the nanopipet tip is approached to the WE sequentially at a series of predefined locations, and upon each landing, a CV is recorded. The *E-t* waveform applied herein is shown in Figure 2b-i; upon landing *E* is initially held at –0.7 V for 5 seconds to 'collect' (reduce) Ag^+ in solution (analogous to the pre-electrolysis step in anodic stripping voltammetry[31]), before sweeping between –0.7 to +0.4 V at 0.1 V s^{-1} to detect Ag^+ through voltammetric stripping analysis. Examples of CVs measured for a carefully positioned QRCE (black trace) and where a fragment of AgCl was deliberately dislodged (red trace) at a GC WE are shown in Figure 2b-ii. For the red trace, the reductive process at $E < -0.45$ V and sharp oxidative peak at $E \approx +0.1$ V are attributable to Ag^+ reduction and Ag^0 oxidation, respectively. As reported below in more detail, the latter response was only observed for a damaged QRCE, and such damage is easily avoided.

Herein, the end of the Ag/AgCl QRCE was consistently positioned approximately 3 cm from the end of the nanopipet probe, as shown in the Supporting Information, Figures S1a and b. A simple 'back-of-the-envelope' calculation of diffusion time[31], assuming a distance of 3 cm and a diffusion coefficient of approximately 1.65×10^{-5} cm^2 s^{-1},[40] indicates that Ag/AgCl contamination should only be a problem on the tens of hours timescale. Yet, the experimental set up used herein is analogous to that employed by Perera and Rosenstein[25], who claimed to have observed Ag/AgCl contamination (*i.e.*, *in situ* metallic nanoparticle formation) after only 40 minutes of operation.

CVs obtained at various times under both ambient and O_2-free (Ar atmosphere) conditions are shown in Figure 3a and b, respectively. Clearly, there is no evidence of Ag/AgCl contamination on the several hours timescale in the presence or absence of O_2, with featureless CVs (background current << 1 pA) being recorded at times up to at least 323 minutes. As highlighted above, these CVs were obtained using a hopping mode protocol, and a total of 400 CVs were recorded over the entire time period, all of which were featureless, as shown in the Supporting Information, Figure S2a. This observation is in agreement with the 'back-of-the-envelope' calculation above, and is consistent with previous work by our group, where no evidence of Ag/AgCl contamination has ever been detected through electrochemistry or microscopy, even with prolonged scanning times.[18,34,43,44] It should also be noted that Ag/AgCl QRCEs are widely employed in SICM, a nanopipet-based technique commonly used for live cell imaging on the several hours to days timescale,[9,23] which would likely not be possible if significant amounts of cytotoxic Ag^+ was being readily released into the growth medium from the end of the probe.

For the above studies, care was taken during preparation and mounting of the nanopipet to avoid physical detachment of any AgCl from the QRCE. If such precautions are not taken, Ag/AgCl contamination is expected on a much smaller timescale, which was emulated here by

purposely bending and distorting the QRCE when inserting it into the nanopipet probe, such that a small piece of AgCl broke off and lodged in the neck of the nanopipet, approximately 150 μm from the tip, as shown in the Supporting Information, Figure S1c. An identical set of hopping-CV experiments were carried out with this probe, with the results shown in Figure 3c. In contrast to the results discussed above, evidence of Ag/AgCl contamination is obvious from the very beginning of the scan, with the Ag^+ reduction/Ag^0 stripping processes evident in the CV recorded at t = 8.3 min (note that the time between probe preparation and recording the first CV at t = 0 min was approximately 30 minutes). The anodic stripping current feature develops to a final charge, Q_{dep}, of ca. 350 fC after *ca.* 160 minutes and subsequent times thereafter. Given that deposition occurs during the collection time of 5 s and during the voltammetric sweep, at potentials negative of *ca.* –0.45 V (giving a total deposition time, t_{tot}, of ca. 7.5 s, prior to the anodic stripping peak) and that the mass transport rate, k_t, in SECCM is approximately 10% of that for the equivalent disc electrode,[26,45] we can estimate the concentration of Ag^+ at the end of the tip, c_{Ag+} as, $Q_{dep} = (4/10)\mathrm{F}Dac_{Ag+}t_{tot}$, (where a is the nanopipet radius), giving $c_{Ag+} \approx 14$ μM, *i.e.*, similar to the concentration expected of a AgCl-saturated solution (see above), which defines the absolute upper bound of the concentration and flux of Ag^+ that can be expected.

The full set of 400 CVs recorded over a 623 min time period are shown in the Supporting Information, Figure S2c. Most of these are very similar to those shown in Figure 3, but also evident in some of the CVs (*ca.* 35%) are oxidative and reductive current 'spikes' attributable to the oxidation of Ag nanoparticles (NPs) and reduction of AgCl NPs, respectively, *i.e.*, nanoparticle impact coulometry.[14] An analysis of the spikes of one CV trace is shown in Figure S3; assuming the current spikes correspond to the complete oxidation of spherical AgCl NPs, diameters (d_{NP}) of just 3.6, 6.1 and 5.3 nm were calculated for the spikes located at –0.380, –0.539 and –0.606 V, respectively.

The CVs obtained with the damaged Ag/AgCl QRCE (Figure 3c) qualitatively resemble those reported by Perera and Rosenstein[25], albeit with much lower measured currents (they measured pA level currents with 'spikes' of tens of pA) and may serve as an explanation as to why they observed contamination artifacts on the 40 minute timescale. We have shown experimentally that Ag/AgCl contamination at the WE does not occur within at least 6 hours when suitable care is taken (*i.e.*, 3 cm placement, no damage to QRCE). Given that 6 hours is likely to be longer than the 'lifetime' of the nanopipet probe, which are usually disposed of after a single set of experiments, it is clear that such contamination artifacts are not important in SECCM, SICM or related nanopipet studies. To further confirm this, transport of Ag^+ from the QRCE to the WE surface (or into bulk solution in the case of SICM) is explored below with FEM simulations.

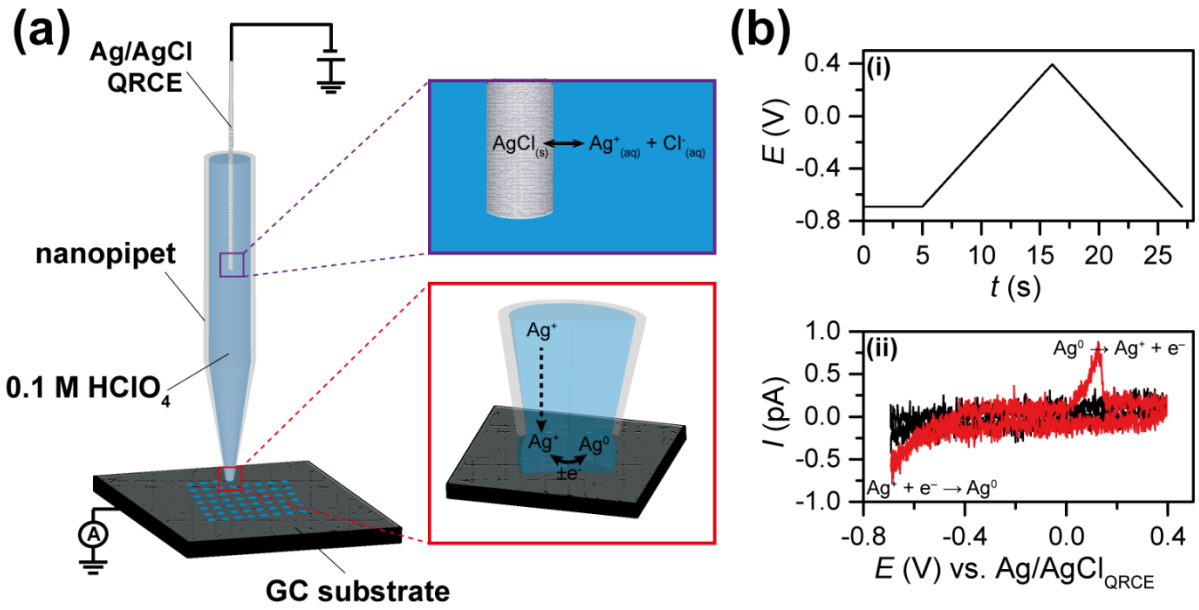

Figure 2. (a) Schematic of the SECCM set up used to test the effect of Ag/AgCl contamination in confined electrochemical cells at prolonged experimental timescales. Shown inset is Ag/AgCl dissolution at the QRCE (purple box) and Ag^+ deposition/Ag^0 stripping at the WE surface (red box). **(b-i)** *E-t* waveform applied at each point (pixel) during the hopping protocol. **(b-ii)** Example CVs obtained at a GC electrode in the absence (black trace) and presence (red trace) of trace Ag^+ (from AgCl dissolution at a detached AgCl fragment). The CVs were obtained with the following experimental parameters: $[HClO_4] = 0.1$ M, voltammetric scan rate (v) = 0.1 V s^{-1}, tip diameter (d_t) ≈ 100 nm and measurement time constant (t_c) = 10 ms.

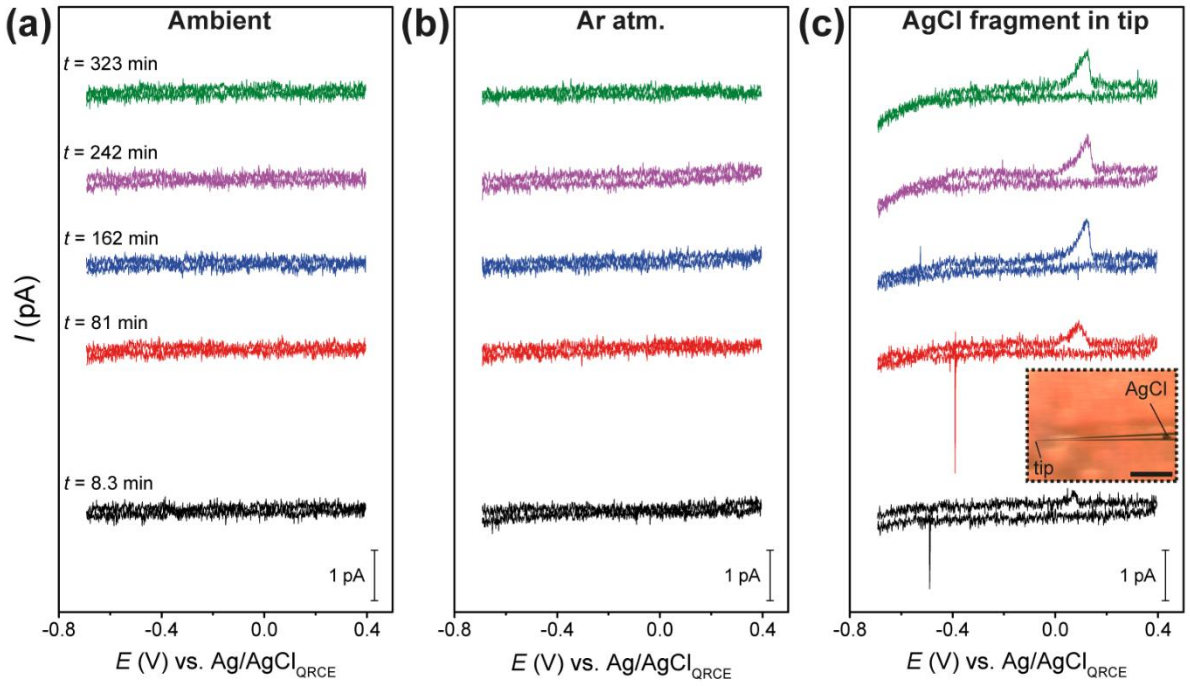

Figure 3. CVs obtained at a GC electrode in the **(a)** presence and **(b)** absence of O_2. **(c)** CVs obtained with a 'contaminated' nanopipet probe that has a fragment of Ag/AgCl located 150 μm from the tip. Shown inset is an optical micrograph of the end of the contaminated probe (scale bar indicates 50 μm). In **(a-c)**, black, red, blue, pink and green traces were obtained at times (t) of 8.3, 81, 162, 242 and 323 min, respectively. Each CV was obtained on a 'fresh' GC surface (*i.e.*, each measurement was independent of the previous). The CVs were obtained with the following experimental parameters: $[HClO_4]$ = 0.1 M, v = 0.1 V s^{-1}, $d_t \approx$ 100 nm and t_c = 10 ms.

Finite element method simulations. To further understand the transport of Ag^+ within the nanopipet probe, FEM simulations of the SECCM (single channel) and SICM configurations were carried out. Full details of the performed simulations are presented in the Supporting Information, Section S2, and some of the key results are shown in Figure 4. It is important to note that Ag^+ is not produced electrochemically at Ag/AgCl QRCEs under typical use conditions (*i.e.*, the electrochemical flux of Ag^+ is equal to zero):

$$AgCl_{(s)} + e^- \rightleftharpoons Ag_{(s)} + Cl^- \qquad (4)$$

In addition, the electrochemical flux of Cl^- at the QRCE if acting as cathode to the WE anode (or if the tip is biased negatively to the bulk in SICM), is negligible/null compared to the passive dissolution flux. For instance, applying a constant cathodic current of 1 nA at the QRCE (corresponding to a current density of 4×10^{-6} mA cm^{-2}, assuming wire diameter and length of 0.025 and 3 cm, respectively) gives rise to a Cl^- concentration of *ca.* 0.4 μM at the QRCE surface, at a time of 1000 seconds (diffusion layer thickness, $\delta \approx \sqrt{2Dt} \approx 2000$ μm)[31], which is negligible compared to that from passive AgCl dissolution (*ca.* 15 μM, see above).

In the SECCM simulations, three conditions were considered at the substrate (WE) surface: (*i*) no flux boundary condition; (*ii*) $[Ag^+]_{surf} = 0$ and; (*iii*) initially a no flux boundary and then switching to $[Ag^+]_{surf} = 0$ after 2, 5 or 20 hours. Situation (*i*) is shown in Figure 4a, which considers $[Ag^+]_{surf}$ *vs.* time when no reaction is occurring (*i.e.*, potential is held at values positive of 0 V, see Figure 2). Evidently, at a QRCE-WE distance (d_{elec}) of 3 cm, no detectable amount of Ag^+ (*i.e.*, sub nM) reaches the WE surface for several hours. It is worth mentioning that the simulated diffusion time is shorter than expected based on the simple back-of-the-envelope calculation carried out above; this is due to radial diffusion effects (*i.e.*, enhanced mass transport) resulting from the tapered geometry of the nanopipet probe.[33,37] Situation (*ii*) is shown in Figure 4b, which considers the substrate (WE) current (I_{sub}) *vs.* time when a reaction is occurring at the mass-transport controlled limit (*i.e.*, the WE is an Ag^+ sink at a 'collection'

potential of –0.7 V). Again, at d_{elec} = 3 cm, several hours pass before Faradaic current (*i.e.*, fA level) attributable to Ag^+ reduction is detectable at the substrate WE. Situation (*iii*) is shown in Figure 4c, which considers the I_{sub} transient measured after 'equilibration times' of 2, 5 and 20 hours. Again, negligible Faradaic current attributable to Ag^+ deposition (fA decaying to tens of aA, well below the measureable limit) is predicted after 2 and 5 hours of equilibration time.

It should be noted that the simulations outlined above only consider mass-transport by diffusion; further simulations (Supporting Information, Figure S5) show that this is a reasonable assumption on the experimental timescales considered herein, with electrical migration effects only becoming significant at prolonged times [>5 hours for d_{elec} = 3 cm and case (ii)]. In addition, migration can only make a significant contribution to Ag^+ transport when a cathodic potential is maintained at the WE [*i.e.*, the WE is an Ag^+ sink, case (*ii*) above], which is often not representative of "real" nanoelectrochemical experiments, where the direction of the electric field is periodically reversed ('flipped') due to pulsing or cycling of the applied potential. Additional discussion is available in the Supporting Information, Section S2.

In the SICM simulations, a bias of +100 mV was applied at the electrode located in the nanopipet and the flux of Ag^+ at the orifice of the probe (*i.e.*, the tip) was calculated as a function of time, as shown in Figure 4d. Again, as is the case above, at d_{elec} = 3 cm, several hours pass before elevated [Ag^+] is detectable at the tip of the nanopipet probe. Interestingly, comparing Figures 4a and d, it is clear that [Ag^+] is an order of magnitude lower in the SICM (*ca.* 0.1 μM at 20 hours) format compared to the SECCM format (*ca.* 2 μM at 20 hours); this is due to the rapid transport of Ag^+ from the probe into bulk solution, which effectively depletes Ag^+ in the vicinity of the probe tip.

Overall, these numerical predictions (and those above) are in excellent agreement with the experimental observations, again indicating that Ag/AgCl contamination is not a consideration for nanopipet experiments in the SICM or SECCM format. $HClO_4$ has solely

been considered as 'model' Cl^- free electrolyte media herein, however it is worth underscoring how other solution conditions may affect Ag/AgCl QRCE stability and contamination. As noted above, E_{QRCE} is set by a_{Cl^-} (approximated by $[Cl^-]$ in Cl^- containing media and set by K_{sp} in Cl^- free media) and can be affected by interfering species such as Br^- (Ag/AgBr would be the more appropriate QRCE in Br^- containing media). Ag/AgCl contamination effects are expected to be exacerbated under conditions where Ag^+ has increased solubility, most notably in Cl^- containing media such as KCl and biological buffers (commonly employed in SICM[10,22,46]), where the formation of soluble $[AgCl_x]^{1-x}$ complexes is possible (*e.g.*, the stability constant, K_{stab} of $[AgCl_2]^-$ is 1.4×10^5 at 298 K in aqueous media).[47] Indeed, this is becoming an increasingly important consideration as nanopipet techniques are being readily adopted for non-aqueous applications (*i.e.*, aprotic solvents[48,49] or ionic liquids[50] in battery electrolytes), where AgCl can possess significant solubility[51] or the formation of $[AgCl_x]^{1-x}$ complexes is thermodynamically very favorable (*e.g.*, the K_{stab} of $[AgCl_2]^-$ is *ca.* 10^{12} in dimethyl sulfoxide[52]). Nevertheless, it needs to be reiterated that experimental timescale is the most critical factor when considering a particular QRCE for an application, irrespective of solution conditions; recent advances have allowed nanoelectrochemical experiments to be carried out on the sub-hour timescale (*e.g.*, high speed scanning approaches in SICM[20,22,46] or SECCM[19,21,45]), where potential instability and Ag^+/Cl^- contamination effects are likely to be insignificant.

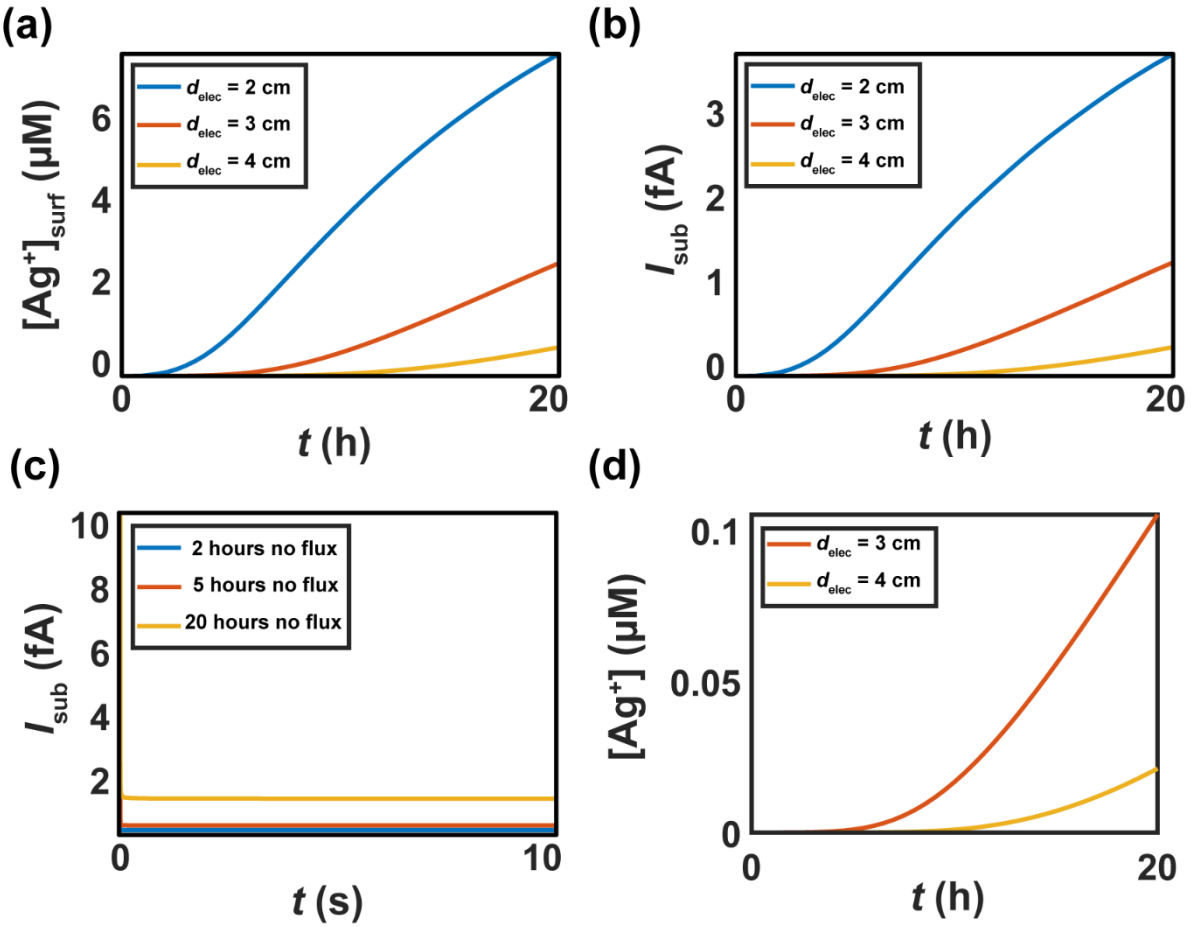

Figure 4. FEM simulations of the SECCM configuration that consider three conditions at the substrate surface: **(a)** no flux boundary condition ($[Ag^+]_{surf}$ *vs.* time); **(b)** $[Ag^+]_{surf} = 0$ (Ag^+ sink condition, I_{sub} *vs.* time) and **(c)** initially a no flux boundary condition applied before switching to $[Ag^+]_{surf} = 0$ after 2, 5 or 20 hours (I_{sub} transient *vs.* time, d_{elec} = 3 cm). The blue, orange and yellow traces correspond to d_{elec} of 2, 3 and 4 cm in **(a-b)**. The blue, orange and yellow traces correspond to equilibration times of 2, 5 and 20 hours in **(c)**. **(d)** FEM simulations of the SICM configuration that consider the flux of Ag^+ at the orifice of the probe when a bias of +100 mV is applied at the electrode located in the nanopipet. The orange and yellow traces correspond to d_{elec} of 3 and 4 cm in **(d)**.

Conclusions

The stability and fouling characteristics of Ag/AgCl QRCEs was investigated in a confined electrochemical cell environment (*i.e.*, nanopipet) at prolonged measurement times (*i.e.*, several hours timescale). The reference potential of freshly-prepared Ag/AgCl QRCEs was found to be very stable in Cl^- free electrolyte media (0.1 M $HClO_4$) when confined within a nanopipet probe in the SICM format, drifting at a rate of *ca.* 1 mV h^{-1} over a 6.5 hour time period. Contrary to a previous report[25], WE fouling by soluble redox by-products (*e.g.*, Ag^+) originating from Ag/AgCl QRCEs was not found to occur after at least 6 hours of scanning in the SECCM configuration as long as suitable precautions with respect to electrode handling (to prevent physical detachment of AgCl) and placement (at least 3 cm from the end of the nanopipet tip) were observed. These experiments were supported by FEM simulations, which consider the transport of Ag^+ within a nanopipet probe in the SECCM and SICM configurations. This work serves as a confirmation that Ag/AgCl is a stable and robust QRCE when confined to a nanopipet probe, a conclusion supported by the widespread use of this important reference electrode system in the field of nanoelectrochemistry and beyond. If handled appropriately, this electrode can be used with confidence as a QRCE in a two-electrode configuration.

Finally, we note that an advantage of pipet-based cells is that one can easily assess the relative importance of ohmic effects in the confined solution, by measuring the conductance current-voltage characteristics.[37] For most SECCM measurements, with mM levels of redox-active species and supporting electrolyte concentrations that are usually two orders-of-magnitude higher, such effects are negligible for voltammetric measurements (which usually show pA to tens of pA current levels).[17,26] Should the redox flux, and associated currents be much higher such that ohmic effects or polarization of the QRCE are no longer negligible, then one can readily adopt a three-electrode SECCM arrangement.[36]

Associated Content

Supporting information. In Section S1, images showing position of QRCE relative to the end of the nanopipet probe tip (Figure S1); CVs (400 total) obtained during the SECCM hopping mode protocol with uncontaminated and contaminated probes (Figure S2); analysis of the transient current spikes recorded in the presence of trace Ag^+ (Figure S3). In Section S2, full details of the FEM simulations (Figures S4 and S5).

Author Information

Corresponding Authors

*C.Bentley.1@warwick.ac.uk (C.L.B.), P.R.Unwin@warwick.ac.uk (P.R.U.)

Notes

The authors declare no competing financial interest.

Acknowledgements

C.L.B. was supported by a Marie Curie Individual Fellowship 702048 NEIL. D.P. was supported by a Leverhulme Trust Research Project Grant. P.R.U. gratefully acknowledges support from a Royal Society Wolfson Research Merit Award.

References

(1) Oja, S. M.; Wood, M.; Zhang, B. *Anal. Chem.* **2013**, *85*, 473-486.

(2) Oja, S. M.; Fan, Y.; Armstrong, C. M.; Defnet, P.; Zhang, B. *Anal. Chem.* **2016**, *88*, 414-430.

(3) Xiao, X. Y.; Fan, F. R. F.; Zhou, J. P.; Bard, A. J. *J. Am. Chem. Soc.* **2008**, *130*, 16669-16677.

(4) Dunevall, J.; Fathali, H.; Najafinobar, N.; Lovric, J.; Wigström, J.; Cans, A.-S.; Ewing, A. G. *J. Am. Chem. Soc.* **2015**, *137*, 4344-4346.

(5) Li, X.; Dunevall, J.; Ewing, A. G. *Acc. Chem. Res.* **2016**, *49*, 2347-2354.

(6) Byers, J. C.; Nadappuram, B. P.; Perry, D.; McKelvey, K.; Colburn, A. W.; Unwin, P. R. *Anal. Chem.* **2015**, *87*, 10450-10456.

(7) Lemay, S. G.; Kang, S.; Mathwig, K.; Singh, P. S. *Acc. Chem. Res.* **2013**, *46*, 369-377.

(8) Novak, P.; Shevchuk, A.; Ruenraroengsak, P.; Miragoli, M.; Thorley, A. J.; Klenerman, D.; Lab, M. J.; Tetley, T. D.; Gorelik, J.; Korchev, Y. E. *Nano Lett.* **2014**, *14*, 1202-1207.

(9) Zhu, C.; Shi, W.; Daleke, D. L.; Baker, L. A. *Analyst* **2018**, *143*, 1087-1093.

(10) Page, A.; Kang, M.; Armitstead, A.; Perry, D.; Unwin, P. R. *Anal. Chem.* **2017**, *89*, 3021-3028.

(11) Shi, W.; Friedman, A. K.; Baker, L. A. *Anal. Chem.* **2017**, *89*, 157-188.

(12) Kang, M.; Perry, D.; Kim, Y.-R.; Colburn, A. W.; Lazenby, R. A.; Unwin, P. R. *J. Am. Chem. Soc.* **2015**, *137*, 10902–10905.

(13) Bentley, C. L.; Kang, M.; Unwin, P. R. *J. Am. Chem. Soc.* **2016**, *138*, 12755-12758.

(14) Ustarroz, J.; Kang, M.; Bullions, E.; Unwin, P. R. *Chem. Sci.* **2017**, *8*, 1841-1853.

(15) Kranz, C. *Analyst* **2014**, *139*, 336-352.

(16) Kang, M.; Momotenko, D.; Page, A.; Perry, D.; Unwin, P. R. *Langmuir* **2016**, *32*, 7993-8008.

(17) Bentley, C. L.; Kang, M.; Unwin, P. R. *Curr. Opin. Electrochem.* **2017**, *6*, 23-30.

(18) Bentley, C. L.; Kang, M.; Maddar, F. M.; Li, F.; Walker, M.; Zhang, J.; Unwin, P. R. *Chem. Sci.* **2017**, *8*, 6583-6593.

(19) Bentley, C. L.; Kang, M.; Unwin, P. R. *J. Am. Chem. Soc.* **2017**, *139*, 16813-16821.

(20) Kang, M.; Perry, D.; Bentley, C. L.; West, G.; Page, A.; Unwin, P. R. *ACS Nano* **2017**, *11*, 9525-9535.

(21) Bentley, C. L.; Unwin, P. R. *Faraday Discuss.* **2018**, DOI: 10.1039/c8fd00028j.

(22) Page, A.; Perry, D.; Young, P.; Mitchell, D.; Frenguelli, B. G.; Unwin, P. R. *Anal. Chem.* **2016**, *88*, 10854-10859.

(23) Miragoli, M.; Moshkov, A.; Novak, P.; Shevchuk, A.; Nikolaev, V. O.; El-Hamamsy, I.; Potter, C. M. F.; Wright, P.; Kadir, S.; Lyon, A. R.; Mitchell, J. A.; Chester, A. H.; Klenerman, D.; Lab, M. J.; Korchev, Y. E.; Harding, S. E.; Gorelik, J. *J. R. Soc. Interface* **2011**, *8*, 913-925.

(24) Yakushenko, A.; Mayer, D.; Buitenhuis, J.; Offenhausser, A.; Wolfrum, B. *Lab Chip* **2014**, *14*, 602-607.

(25) Perera, R. T.; Rosenstein, J. K. *Scientific Reports* **2018**, *8*, 1965.

(26) Ebejer, N.; Güell, A. G.; Lai, S. C. S.; McKelvey, K.; Snowden, M. E.; Unwin, P. R. In *Annual Review of Analytical Chemistry, Vol 6*, Cooks, R. G.; Pemberton, J. E., Eds.; Annual Reviews: Palo Alto, 2013, pp 329-351.

(27) Li, M.; Li, Y.-T.; Li, D.-W.; Long, Y.-T. *Anal. Chim. Acta* **2012**, *734*, 31-44.

(28) Sze, J. Y. Y.; Ivanov, A. P.; Cass, A. E. G.; Edel, J. B. *Nat. Commun.* **2017**, *8*, 10.

(29) Page, A.; Perry, D.; Unwin, P. R. *Proc. Royal Soc. A* **2017**, *473*.

(30) Chen, C.-C.; Zhou, Y.; Baker, L. A. *Annu. Rev. Anal. Chem.* **2012**, *5*, 207-228.

(31) Bard, A. J.; Faulkner, L. R. *Electrochemical Methods : Fundamentals and Applications*, 2nd ed.; Wiley: New York, 2001, p 833.

(32) Janz, G. J.; Ives, D. J. G. *Ann. N. Y. Acad. Sci.* **1968**, *148*, 210-221.

(33) Snowden, M. E.; Güell, A. G.; Lai, S. C. S.; McKelvey, K.; Ebejer, N.; O'Connell, M. A.; Colburn, A. W.; Unwin, P. R. *Anal. Chem.* **2012**, *84*, 2483-2491.

(34) Bentley, C. L.; Andronescu, C.; Smialkowski, M.; Kang, M.; Tarnev, T.; Marler, B.; Unwin, P. R.; Apfel, U. P.; Schuhmann, W. *Angew Chem Int Ed Engl* **2018**, *57*, 4093-4097.

(35) Takahashi, Y.; Kumatani, A.; Munakata, H.; Inomata, H.; Ito, K.; Ino, K.; Shiku, H.; Unwin, P. R.; Korchev, Y. E.; Kanamura, K.; Matsue, T. *Nat. Commun.* **2014**, *5*, 1-7.

(36) Mariano, R. G.; McKelvey, K.; White, H. S.; Kanan, M. W. *Science* **2017**, *358*, 1187-1192.

(37) Perry, D.; Momotenko, D.; Lazenby, R. A.; Kang, M.; Unwin, P. R. *Anal. Chem.* **2016**, *88*, 5523-5530.

(38) Williams, C. G.; Edwards, M. A.; Colley, A. L.; Macpherson, J. V.; Unwin, P. R. *Anal. Chem.* **2009**, *81*, 2486-2495.

(39) Dean, J. A.; Lange, N. A. *Lange's Handbook of Chemistry*; McGraw-Hill, 1999.

(40) Macpherson, J. V.; Unwin, P. R. *J. Phys. Chem.* **1995**, *99*, 14824-14831.

(41) Macpherson, J. V.; Unwin, P. R. *J. Phys. Chem.* **1996**, *100*, 19475-19483.

(42) Lai, S. C. S.; Patel, A. N.; McKelvey, K.; Unwin, P. R. *Angew. Chem.* **2012**, *124*, 5501-5504.

(43) Güell, A. G.; Cuharuc, A. S.; Kim, Y.-R.; Zhang, G.; Tan, S.-y.; Ebejer, N.; Unwin, P. R. *ACS Nano* **2015**, *9*, 3558-3571.

(44) Patten, H. V.; Lai, S. C. S.; Macpherson, J. V.; Unwin, P. R. *Anal. Chem.* **2012**, *84*, 5427-5432.

(45) Momotenko, D.; Byers, J. C.; McKelvey, K.; Kang, M.; Unwin, P. R. *ACS Nano* **2015**, *9*, 8942-8952.

(46) Momotenko, D.; McKelvey, K.; Kang, M.; Meloni, G. N.; Unwin, P. R. *Anal. Chem.* **2016**, *88*, 2838-2846.

(47) Fritz, J. J. *J. Solution Chem.* **1985**, *14*, 865-879.

(48) E, S. P.; Kang, M.; Wilson, P.; Meng, L.; Perry, D.; Basile, A.; Unwin, P. R. *Chem. Commun.* **2018**, *54*, 3053-3056.

(49) Snowden, M. E.; Dayeh, M.; Payne, N. A.; Gervais, S.; Mauzeroll, J.; Schougaard, S. B. *J. Power Sources* **2016**, *325*, 682-689.

(50) Aaronson, B. D. B.; Lai, S. C. S.; Unwin, P. R. *Langmuir* **2014**, *30*, 1915-1919.

(51) Kakiuchi, T.; Yoshimatsu, T.; Nishi, N. *Anal. Chem.* **2007**, *79*, 7187-7191.

(52) Luehrs, D. C.; Iwamoto, R. T.; Kleinberg, J. *Inorg. Chem.* **1966**, *5*, 201-204.

For TOC only:

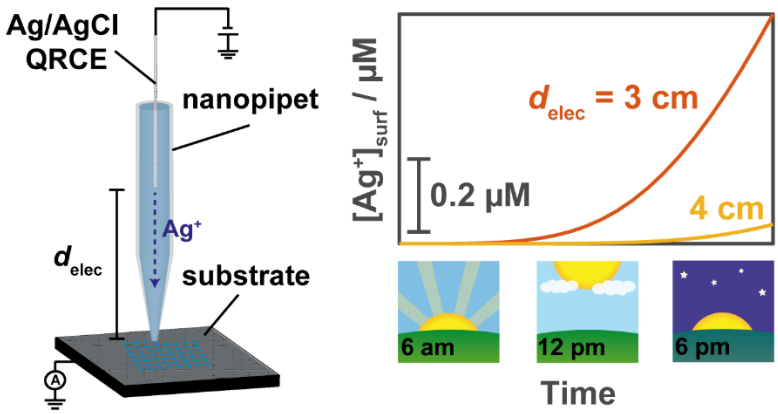
Ag/AgCl
QRCE
nanopipet
Ag+
d elec
substrate
[Ag+]surf / µM
d elec = 3 cm
0.2 µM
4 cm
6 am
12 pm
6 pm
Time